

Experiments on gravity-driven particle flows in a turbulent stream

Tobias Böhm

Cemagref, Dom. Univ. BP 76, 38402 Saint Martin d'Hères Cedex, France, tobias.boehm.1976@web.de

Christophe Ancey

Ecole Polytechnique Fédérale de Lausanne, Ecublens, 1015 Lausanne, Switzerland, christophe.ancey@epfl.ch

Philippe Frey

Cemagref, Dom. Univ. BP 76, 38402 Saint Martin d'Hères Cedex, France, philippe.frey@cemagref.fr

Magali Jodeau

Cemagref, 3 bis quai Chauveau, 69336 Lyon, France, jodeau@lyon.cemagref.fr

Jean-Luc Reboud

Université Joseph Fourier, LEMD, 25 av Martyrs, 38042 Grenoble, France, jean-luc.reboud@grenoble.cnrs.fr

ABSTRACT: Bed load transport in watercourses is a longstanding problem in the mechanics of two-phase flows because the involved physical processes are poorly known or overly complicated. The motion of coarse spherical glass beads entrained by a shallow turbulent water flow down a steep two-dimensional channel with a mobile bed was experimentally investigated. Focus was put on bed load equilibrium flows, that is, neither erosion nor deposition of particles over sufficiently long time intervals occurred. Flows were filmed from the side by a high-speed camera. Using an image processing software made it possible to determine the flow characteristics such as particle trajectories, their state of motion (rest, rolling or saltating motion) and flow depth. Our first striking result was that, over short time periods, bed load transport appeared as a very intermittent process. Whereas for moderate slopes particles were mainly transported in saltation, the rolling regime was dominant for steep slopes.

1 INTRODUCTION

Among two-phase flow problems particular sediment transport in water courses is difficult. Many engineers endeavored to calculate the transport rate as a function of the water flow. Empirical formulas as the Meyer-Peter formula (Meyer-Peter & Müller 1948) were established. Formulas of this type state that bed load transport (particles staying near the river bed without getting into suspension) occurs if the water discharge exceeds a threshold value (Julien 1994). These laws correctly predict the transport rates for steady uniform flows, whereas they yield poor results for more general flow conditions. Furthermore, the theoretical background of these formulas (Bagnold 1973) has been sporadically criticized, notably recently (Seminara et al. 2002).

This explains the interest in a better understanding of the physical mechanisms ruling bed load transport. An approach takes its roots in the probabilistic view

of Einstein (Einstein 1950) who described the sediment transport rate as the difference between an entrainment and a deposition rate. Furthermore, the idea of considering bed load transport not as the flux of a continuous phase but as the superimposition of the motion of individual particles has gained new attention in the last decades [see (Wiberg & Smith 1985) and (Schmeeckle & Nelson 2003)]. The equation of motion is integrated numerically to calculate the trajectories of the particles. But empirical approaches have still to be used to model the forces exerted on the particles since the mechanisms of bed load transport are insufficiently understood.

Our contribution to this issue is based on the idea of reducing bed load transport to its essential elements using a two-dimensional model channel. Initially, the motion of a single particle in a water flow was investigated (Ancey et al. 2002) and (Ancey et al. 2003). In the present study we supplied the channel continu-

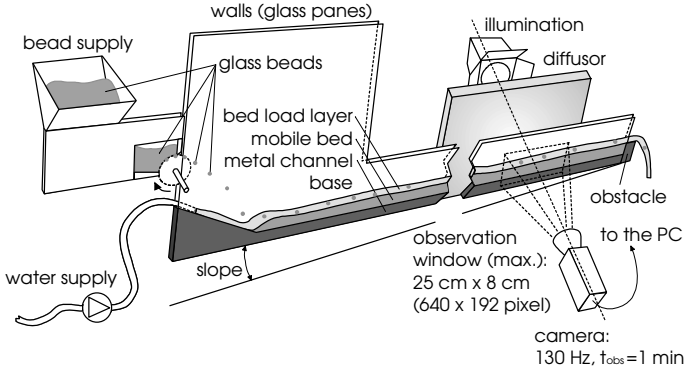


Figure 1. Sketch of the experimental setup. After (Böhm et al. 2004).

ously with sediment (spherical glass beads). We were able to take sophisticated measurements by means of image processing and to analyze the results from a physical point of view. We paid special attention to the mobile bed, i.e. the incessant exchange between the moving particles and the bed. This microstructural study provided a deep insight into transport mechanisms. The results are intended to be used to advance the development of numerical bed load transport models.

The following section describes briefly the experimental facilities and the image and data processing algorithms developed. The results are presented in three subsections: After dealing with the fluctuations of the solid discharge we investigate the influences of flow rate and channel slope on the transport features.

2 EXPERIMENTAL METHOD

Bed load experiments were conducted in a narrow, glass-sided channel, 2 m in length (see Fig. 1). The slope was adjusted ranging from 7.5% to 12.5%. The channel was continuously supplied with water and spherical glass beads with a diameter of 6 mm. As the channel ($W = 6.5$ mm) was only slightly wider than this diameter, the particle motion was approximately two-dimensional. An obstacle at the channel outlet prompted the particles to settle on the rough channel base to form a bed of three particle layers on average. The water flow rate q_w and the particle injection rate \dot{n}_0 were adjusted at the upstream entrance to obtain bed load equilibrium, that is, neither erosion nor deposition of the particle bed over sufficiently long time intervals. Flows were filmed from the side by a high-speed camera allowing to record the motion of a set of particles (about 100 individuals) during approximately one minute. Figure 2 shows typical images.

Images were analyzed using algorithms which combined image-processing operations of the WIMA software provided by the Traitement du Signal et Instrumentation laboratory in Saint-Etienne (France). The water free surface was detected using its slim form; missing portions were inter- or extrapolated. Positions of the bead mass centers were detected by comparing the filmed images with the image of a model bead. The correlation maxima were calculated

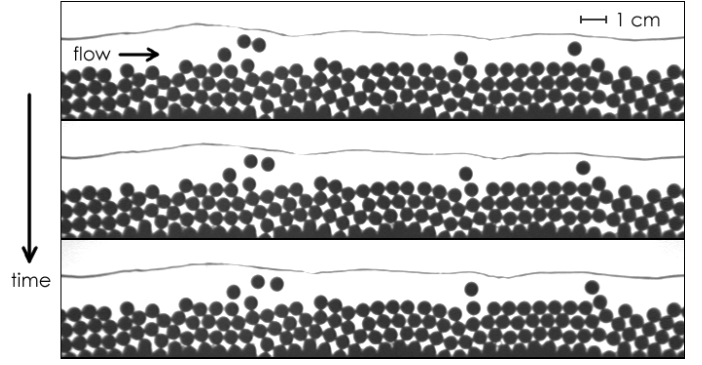


Figure 2. Images of the particle transport. Image dimensions: $25 \text{ cm} \times 5 \text{ cm}$; frame rate: $f = 129.2 \text{ Hz}$, channel inclination: $\tan \theta = 10\%$, mean solid discharge $\dot{n} = 7.93 \text{ beads/s}$, water discharge per unit width $q_w = 5.39 \times 10^{-3} \text{ m}^2/\text{s}$. After (Böhm et al. 2004).

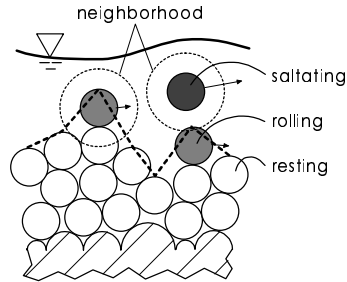


Figure 3. Sketch defining the state of movement and the bed line.

to obtain the bead positions. Resulting uncertainty on the water line and bead positions was less than 1 pixel or 0.4 mm. We developed a particle tracking algorithm to calculate the trajectories of each of the filmed beads step by step. The state of movement of a particle was defined by considering that each bead was either in a resting, rolling or saltating regime (see Fig. 3). We defined resting particles as those with a velocity lower than a threshold value and saltating particles as those without contact to other particles (apart from collisions). The remaining particles were considered to be in the rolling regime. Defining the bed surface profile to be the broken line linking the top points of the uppermost resting or rolling beads made it possible to calculate the water depth h . A paper on the developed algorithms is in preparation (Böhm et al. prep).

3 RESULTS

3.1 Fluctuations of the solid discharge

In preliminary experiments, we measured substantial fluctuations of the solid discharge. We express the solid discharge in beads per second and define it as:

$$\dot{n} = \frac{1}{L} \sum_{i=1}^N u_i.$$

L , N , and u_i are the vertical length of the observation window, the number of the observed particles, and the x -component of the individual particle velocity, respectively. The solid discharge represents thus the cumulated motion of the particles in the observation window.

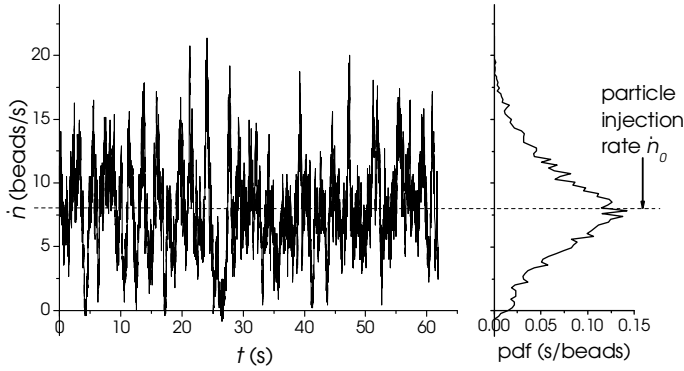


Figure 4. Time variation of the solid discharge. Probability density function of the solid discharge. Experimental conditions: see Figure 2.

Figure 4 shows the time series of \dot{n} for one experiment. The diagram reveals strong fluctuations of the particle transport: While there were phases without transport, the solid discharge maximum was virtually three times the particle injection rate ($\dot{n}_0 = 8$ beads/s). This is illustrated by the probability density function of \dot{n} (Fig. 4), which was wide, bell shaped and nearly symmetric. Despite of the large fluctuations, the mean value of the measured solid discharge ($\dot{n} = 7.93$ beads/s) matched the injection rate very well.

The fluctuations originated from particle liftoff and settling events and from the collective motion of rolling particles. To some extent, these features of the mobile particle bed are illustrated in Figure 2, further comments are provided in (Böhm et al. 2004).

3.2 Influence of the flow rate

Three experiments were run with different particle injection rates by adjusting each time the water discharge in order to obtain bed load equilibrium. In Figure 5 we plotted the distributions of \dot{n} in the vertical direction of the flow [solid curves (1)]. Additionally, we show the individual contribution of the saltating (2), rolling (3), and resting (4) particles to the total solid discharge.

The diagrams showed three peaks at intervals of approximately one particle diameter. Figure 5c revealed a fourth peak one particle diameter above, the transport occupied here a wider y -range, as the water level was higher too. The occurrence of peaks in the transport profiles indicates that the particle bed had a layered structure. This order in the bed developed although we payed special attention to design an irregular channel base (see Fig. 2).

The peaks of Figure 5 coincide fairly with the presence of different transport regimes. In the lower part [small peaks (4)] particles moved at low drift velocities i.e. in the resting regime. Each of the central peaks (3) [for Fig. 5c the two central peaks] represents mostly the contribution of the rolling particles. The uppermost peaks (2) are essentially due to particles in saltation. It is remarkable that the two lower peaks grew only little from a to c while the uppermost peak grew sensibly and produced for Figure 5c a fur-

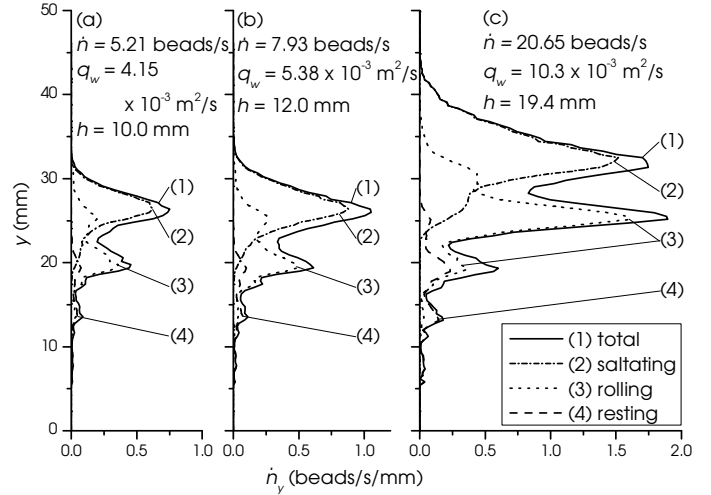


Figure 5. Solid discharge \dot{n}_y as a function of the y -coordinate (total solid discharge and elementary contributions) for three different experiments. Varied parameters: Solid discharge \dot{n} , water discharge q_w , water depth h . Constant parameter: Channel slope $\tan \theta = 10\%$.

ther peak. A higher solid discharge was thus mainly achieved by an increase of the transport near the water free surface, while the particle transport below remained nearly constant.

The y -integrals of the dashed curves represent the weights of the different transport regimes. Here, the three experiments differed barely: The contribution of the saltating (2), rolling (3), and resting (4) particles to the solid discharge was 51–55%, 38–41%, and 6–8%, respectively.

3.3 Influence of the channel slope

Next we ran three experiments with different channel slopes keeping the solid discharges approximately constant. The water discharge q_w was however adapted for each experiment to establish bed load equilibrium. Increasing the slope from 7.5% to 12.5%, q_w had to be decreased by a factor 4.6, which involved also a reduction of the water depths h .

The features of the particle transport at different slopes are illustrated in Figure 6. To obtain these diagrams we counted for each pixel of the observation window the number of particles, N' , that passed during the sequence. In other words the diagrams represent the superimposition of the particle trajectories by the number N' coded in gray levels. It is striking that the rolling particles in the lower part followed specific paths. At certain (x, y) -positions more than 100 particles passed. Note that at each x -position (for an arbitrary y) approximately $9 \text{ beads/s} \times 61 \text{ s} \approx 550$ beads passed over the sequence. The diagrams show once again the distinct layer structure of the particle transport.

Several distinctions of the particle transport at different slopes were revealed. At low slope (see Fig. 6a) the saltation was dominant (61.7%). Here, the cited paths of the rolling and sliding beads were relatively little frequented (maximal value $N' = 95$ beads). In

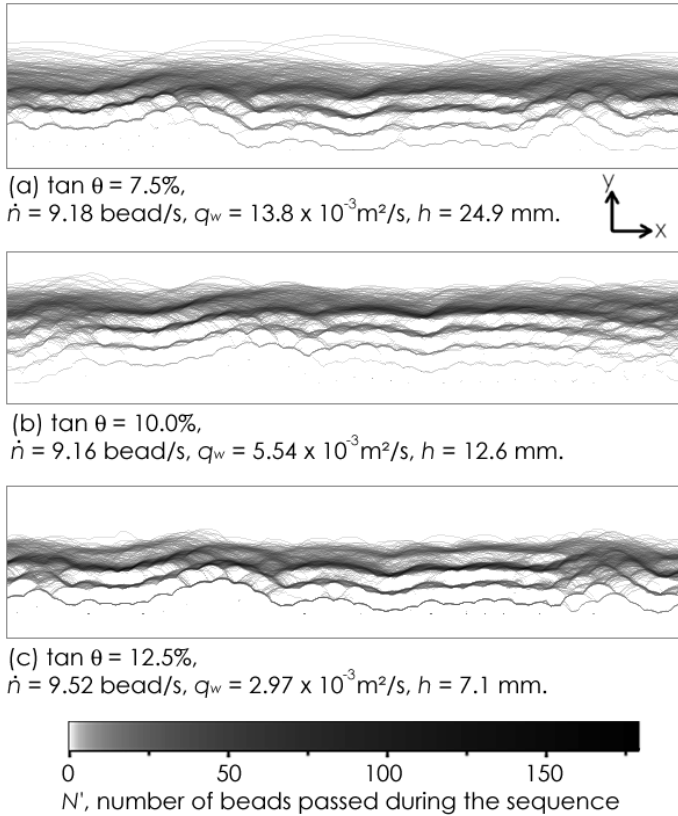


Figure 6. Superimposition of the trajectories for experiments at different slopes $\tan \theta$. Varied parameters: Channel slope $\tan \theta$, water discharge q_w , water depth h . The solid discharge is fairly constant ($\dot{n} \approx 9$ beads/s).

the upper part of the diagram, there was a wide zone of transport where N' took values between 1 and 20 (light gray). This was the zone of saltation. Because of the high water depth, it was rather broad. In the upper part of this zone one can notice several long leaps.

Different is the case of steeper slope (see Fig. 6c). The zone of saltation was narrower and the leaps were noticeably shorter. Here, the beads were predominantly rolling (69.7%) and followed frequently specific paths (see the dark lines in the diagram, the maximum of N' was 175 beads). In short, the diagrams illustrated that the contribution of the rolling particles to the solid discharge raised with the slope.

4 CONCLUSIONS

In this paper, the mechanisms of bed load transport were investigated, using an idealized experimental setup. We measured substantial fluctuations of the solid discharge, which can be attributed to the collective motion of particles. At constant slope, an increase of the solid discharge increased mainly the transport near the water free surface, while the particle transport in the lower part remained nearly constant. For steeper slopes the water depth was reduced to the order of one particle diameter, which forced the particles to stay in mutual contact and displace in the rolling regime.

In our experiments it was crucial to limit the particle motion to two dimensions, which allowed us to

capture the entire motion of a set of particles. This made it possible to gain insight into the transport mechanisms, which are in our opinion essential to develop particle based bed load transport models.

ACKNOWLEDGMENTS

This study was supported by the program ECCO/PNRH of INSU. We are grateful to the laboratory TSI UMR 5516 (Christophe Ducottet, Nathalie Bochar, Jacques Jay, and Jean-Paul Schon).

REFERENCES

- Ancey, C., Bigillon, F., Frey, P., & Ducret, R. 2003. Rolling motion of a bead in a rapid water stream. *Physical Review E* 67: 011303.
- Ancey, C., Bigillon, F., Frey, P., Ducret, R., & Lanier, J. 2002. Saltating motion of a bead in a rapid water stream. *Physical Review E* 66: 036306.
- Bagnold, R. 1973. The nature of saltation and of 'bed load' transport in water. *Proceedings of the Royal Society of London A* 473-504: 332.
- Böhm, T., Ancey, C., Frey, P., Reboud, J., & Ducottet, C. 2004. Fluctuations of the solid discharge of gravity-driven particle flows in a turbulent stream. *Physical Review E* 69: 061307.
- Böhm, T., Ducottet, C., Frey, P., Ancey, C., & Reboud, J. in prep.
- Einstein, H. 1950. The bed-load function for sediment transportation in open channel flows. *Technical Bulletin of the United States Department of Agriculture* 1026.
- Julien, P. 1994. *Erosion and sedimentation*. Press Syndicate of the University of Cambridge.
- Meyer-Peter, E. & Müller, R. 1948. Formulas for bed-load transport. In *Int. Assoc. Hydraul. Res., 2nd meeting, Stockholm*: 39-64.
- Schmeeckle, M. & Nelson, J. 2003. Direct numerical simulation of bedload transport using a local, dynamic boundary condition. *Sedimentology* 50: 279-301.
- Seminara, G., Solari, L., & Parker, G. 2002. Bed load on arbitrarily sloping beds: Failure of the Bagnold hypothesis. *Water Resources Research* 38: 1249.
- Wiberg, P. & Smith, J. 1985. A theoretical model for saltating grains in water. *Journal of Geophysical Research* 90: 7341-7354.